Energy distribution in a scatterplate interferometer

Lawrence F. Rubin and James C. Wyant
Optical Sciences Center, University of Arizona, Tucson, Arizona 85721
(Received 10 February 1979)

In this paper, a Fourier-optics approach to scatterplate interferometry is introduced. In particular, it is used to explain how energy is conserved for both "phase"- and "density"-type scatterplates.

INTRODUCTION

By adding the energy produced in the interferograms and absorbed by the interferometer itself, it must be possible to prove energy conservation in any interferometer. This calculation is relatively simple for two port interferometers such as the Twyman-Green and Mach-Zehnder. If nonabsorbing beam splitters are used, primary and complementary fringe patterns are produced such that when a dark fringe appears in one port a bright fringe appears in the other. The sum of the energy in the two fringe patterns remains a constant. If absorbing beam splitters are used such as thin film aluminum, the two fringe patterns are not necessarily complementary. However, it can be shown that if the energy absorbed by the beam splitter is included in the calculation, the total energy again remains constant. To our knowledge, an analysis showing the distribution of energy in a scatterplate interferometer[1,2] has not been previously given. The purpose of this paper is to present a conservation of energy analysis for both phase and density scatterplate interferometers and in the process provide a description of the operation of a scatterplate interferometer.

QUALITATIVE VIEW OF SCATTERPLATE INTERFEROMETRY

Figure 1 illustrates the optical schematic of a scatterplate interferometer testing a concave surface at its nominal radius of curvature. The important element is the scatterplate itself which is a weak diffuser that possesses a flip or inversion symmetry about a unique point. When focused light from the pinhole passes through the scatterplate, a reference beam (unscattered or direct beam) and a test beam (scattered beam) are formed. Since there is a double passage through the scatterplate, four types of beam amplitudes will combine to give the interferogram in the image plane: DD (direct-direct), light unscattered after two passages through the scatterplate; DS (direct-scattered), light unscattered the first passage and scattered the second passage; SD (scattered-direct), light scattered the first passage and unscattered the second passage;

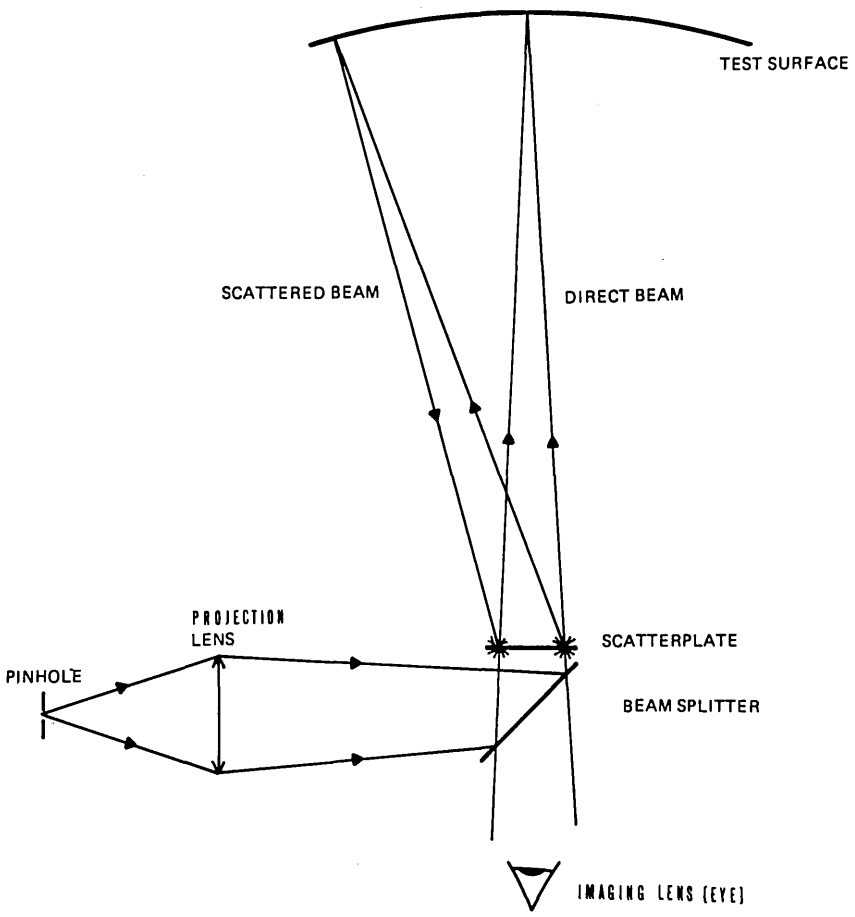

FIG. 1. Schematic of scatterplate interferometer.

 0030-3941/79/091305-04$00.50

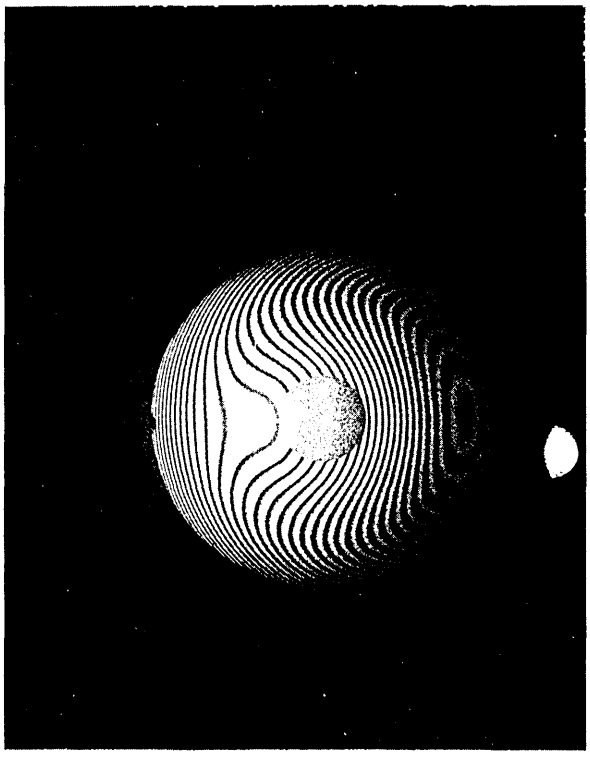

FIG. 2. Scatterplate interferogram obtained testing parabolic mirror.

SS (scattered-scattered), light scattered at both passages.

The fringe contours in the presence of test aberrations are given by the sum of the DS and SD light. The DD light forms the characteristic hotspot while the SS light reduces the fringe contrast by adding a constant background intensity. Figure 2 shows a typical scatterplate interferogram obtained by testing a parabolic mirror. Note the hotspot produced by the DD light and the background speckle pattern resulting from the use of coherent laser light. One method of making scatterplates is by double exposing a laser speckle pattern on a photographic plate and rotating the plate 180° between exposures to obtain the flip symmetry.[3] If the photographic plate is bleached after normal processing, the light will scatter off the phase variations in the emulsion. If the plate is not bleached, the light scatters off silver density variations.

MATHEMATICAL ANALYSIS

A more formal understanding of the scatterplate interferometer can be obtained by unfolding the schematic of Fig. 1 as shown in Fig. 3. Seen in this form, the scatterplate interferometer is not unlike a coherent optical processor. Assuming for simplicity that the scattered light just covers the test aperture, the usual Fourier techniques will show the intensity in the fringe plane to be given by

$$I_f = I_0|e^{ikw}[S^+]^{\sim}{**}[S^-]^{\sim}|^2 = I_0|[([e^{ikw}]^{\sim}{**}S^+)S^-]^{\sim}|^2 \tag{1}$$

where w is the aberration in the test lens, $k = 2\pi/\lambda$, S is the scatterplate amplitude transmission, $[S]^{\sim}$ is the Fourier transform of S, I_0 is the incident intensity on the first scatterplate which will be set equal to 1, and ** denotes a two-dimensional convolution.

Since the first scatterplate is imaged inverted at the second plate, a + or − superscript is placed on S to denote this inversion. For the following analysis, perfect flip symmetry in the scatterplate will be assumed so that

$$S^+ = S^- = S. \tag{2}$$

The particular form for S depends on whether the scatterplate is a density or phase type.

Considering only surface height variations, the phase scatterplate transmission amplitude can be written as

$$S_p = A\exp[ik(n-1)h], \tag{3}$$

where A is the scatterplate aperture function, n is the emulsion index of refraction, and h is the emulsion surface height variations referenced to a zero mean.

The variations in h are usually small enough to consider only the first two terms of the exponential expansion

$$S_p \approx A[1 + ik(n-1)h]. \tag{4}$$

Use of Eq. (4) simplifies the understanding of the algebra that follows its substitution into Eq. (1). However, it should be pointed out that this approximate expression has a modulus greater than the exact form shown in Eq. (3). The Fourier transform of Eq. (4) can be written as

$$[S_p]^{\sim} = [A]^{\sim}{**}\{\delta + ik(n-1)[h]^{\sim}\}, \tag{5}$$

where δ is the Dirac delta function centered at the origin. For a density scatterplate

$$S_D = A[t_0 + t_1] \tag{6}$$

and

$$[S_D]^{\sim} = [A]^{\sim}{**}(t_0\delta + [t_1]^{\sim}) \tag{7}$$

where t_0 is the average transmission and t_1 is the variations in transmission about the mean t_1.

In order to investigate energy conservation in the scatterplate interferometer, it would be desirable to obtain a null fringe across the test aperture. However, the conventional scatterplate is a common-path interferometer and if a perfectly spherical optical surface is tested, there is zero piston error between the reference and test beams and it is impossible to obtain a null fringe. Of course, if the direct beam (hotspot) should happen to focus on a small bump or hole on the mirror surface, a null fringe would be possible. Since in both the analysis and experiment we wanted to be able to vary the relative phase of the SD and DS beams, a modified scatterplate interferometer shown in Fig. 4 was constructed. Now the reference beam is reflected off a remote mirror mounted on a piezoelectric crystal. By applying a voltage across the PZT, piston error is introduced just as if this mirror were placed in one of the beams of a Twyman-Green interferome-

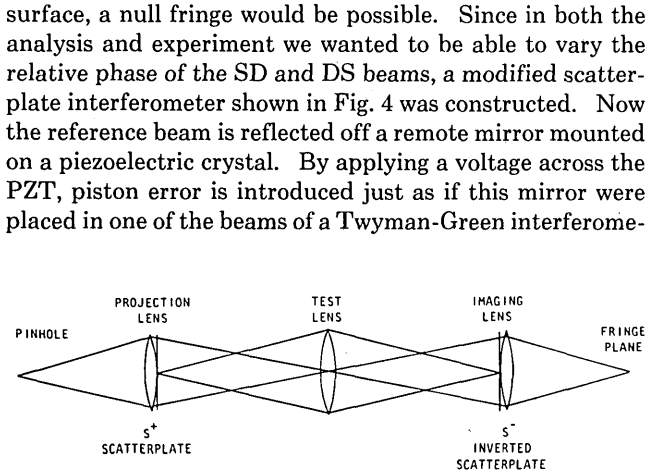

FIG. 3. Unfolded schematic of a scatterplate interferometer.

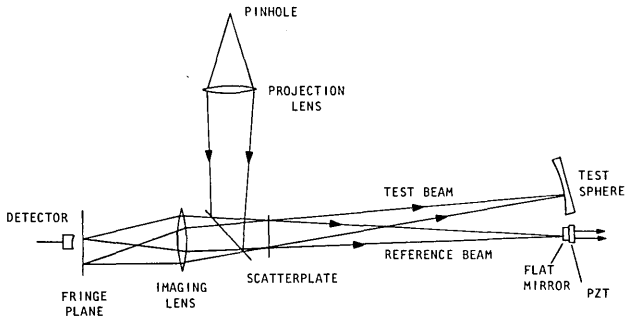

FIG. 4. Schematic of a scatterplate interferometer used in noncommon path mode.

ter. Since the remote mirror phase shifts only the unscattered light, the new forms for S_p^+ and S_D^+ will be

$$S_p^+ = A[e^{i\phi} + ik(n-1)h], \tag{8}$$

$$S_D^+ = A[e^{i\phi}t_0 + t_1], \tag{9}$$

where ϕ is the phase shift introduced by the remote mirror. The S_p^- and S_D^- terms do not contain the $e^{i\phi}$ term since they are unaffected by the remote mirror. We do not imply by the retention of the superscripts that new forms for S_p and S_D are not inversion symmetric. In the following analysis, they are used to label the first and second passages through the scatterplate itself.

Substituting Eq. (4) for S_p^- and Eq. (8) for S_p^+ into Eq. (1),

$$I_f = |A^2]\sim e^{i(\phi)} + ik(n-1) \times (e^{ikw}[Ah]\sim)^{**}[A]\sim + i[A^2]\sim h e^{i\phi}k(n-1) - k^2(n-1)^2(e^{ikw}[Ah]\sim)^{**}[Ah]\sim|^2, \tag{10}$$

where the relation $[A]\sim^{**}[h]\sim = [Ah]\sim$ has been used. It is assumed for simplicity that W is slowly varying compared to $[A]\sim$, the Airy pattern of the scatterplate aperture. Before squaring the above expression, it is useful to point out that terms inside the brackets are the DD, SD, DS, and SS amplitude mentioned earlier. Using the fact that symmetric functions give real transforms

$$I_f = [A]\sim\{[A]\sim + 2k(n-1)[Ah]\sim\sin(\phi - kw) - 2k^2(n-1)^2\mathrm{Re}\{e^{i\phi}B^*\} + 2k^2(n-1)^2[1+\cos(kw-\phi)]([Ah]\sim)^2 + k^4(n-1)^4|B|^2 - 2k^3(n-1)^3[Ah]\sim\mathrm{Re}\{ie^{i\phi}B^*\} - 2k^3(n-1)^3[Ah\sim]\mathrm{Re}\{ie^{ikw}B^*\}, \tag{11}$$

where $B = (e^{ikw}[Ah]\sim)^{**}[Ah]\sim$, $A = A^2$ for zero or one type apertures, and Re{ } is the real part of { }.

The first three terms are grouped together to form the hotspot intensity, I_{DD}. They are a combination of not only the DD amplitude squared but also the SD and SS amplitudes scattered in the direction of the hotspot. The fourth term represents the signal term I_S which results from the interference of the SD and DS amplitudes, the test and reference beams. In the scatterplate fabrication, the accuracy to which the 180° rotation is achieved has a strong effect on the contrast of the fringe contours given by I_S. Finally the last three terms are the background intensity, which are the interference terms between the SS and DS amplitudes.

Setting $W = 0$, I_f reduces to

$$I_f = [A]\sim([A]\sim + 2k(n-1)[Ah]\sim\sin\phi - 2[Ah^2]\sim k^2(n-1)^2\cos\phi)\ \}I_{DD} + 2k^2(n-1)^2(1+\cos\phi)([Ah]\sim)^2\ \}I_S + k^4(n-1)^4([Ah^2]\sim)^2 + 2k^3(n-1)^3 \times [Ah]\sim[Ah^2]\sim\sin\phi\ \}I_{SS}. \tag{12}$$

Integrating I_f over the image plane gives the power transfer among the variant terms,

$$\int I_f dA_I = A_S - 2k^2(n-1)^2A_S\langle h^2\rangle\cos\phi\ \}\text{hotspot} + 2k^2(n-1)^2A_S\langle h^2\rangle(1+\cos\phi)\ \}\text{signal} + k^4(n-1)^4A_S\langle h^4\rangle\ \}\text{background}, \tag{13}$$

$$= A_S + 2k^2(n-1)^2A_S\langle h^2\rangle + k^4(n-1)^4A_S\langle h^4\rangle, \quad \text{independent of } \phi, \tag{14}$$

where $\langle\ \rangle \equiv$ average value, dA_I is the area increment in the image plane, dA_S is the area increment in the scatterplate plane, and Rayleigh's theorem[4]

$$\int [A]\sim[Ah^2]\sim dA_1 = \int AAh^2 dA_S = A_S\langle h^2\rangle. \tag{15}$$

Since I_f is a constant with time, Eqs. (13) and (14) differ from the energy transfer by a constant t_0, the integration time. Notice that the hotspot and signal term oscillate 180° out of phase with variations in ϕ. Equations (13) and (14) show that the energy is transferred between the signal and the hotspot, as a function of ϕ, the background energy being independent of ϕ.

DENSITY SCATTERPLATE

Substituting the expressions (6) and (9) for S_D into (1) setting $W = 0$ gives

$$I_f = [A]\sim(t_0^4[A]\sim + 2t_0^3[At_1]\sim(1+\cos\phi) + 2t_0^2[At_1^2]\sim\cos\phi)\ \}I_{DD} + 2t_0^2([At_1]\sim)^2(1+\cos\phi)\ \}I_S + ([At_1^2]\sim)^2 + 2t_0[At_1]\sim[At_1^2]\sim(1+\cos\phi)\ \}I_{SS}. \tag{16}$$

Again integrating I_f over A_I gives the power transfer among the hotspot, signal, and background terms as a function of ϕ,

$$\int I_f dA_I = t_0^4A_S + 2t_0^2A_S\langle t_1^2\rangle\cos\phi\ \}\text{hotspot} + 2t_0^2A_S\langle t_1^2\rangle(1+\cos\phi)\ \}\text{signal} + \langle t_1^4\rangle\ \}\text{background}. \tag{17}$$

There still is no net energy transfer to the background, but now the hotspot and signal terms are oscillating in phase with ϕ rather than 180° out of phase as before. Physically, the hotspot intensity is a combination of the DD amplitude (which is phase shifted ϕ by the PZT mirror) and the SS amplitude scattered in the direction of the hotspot. The difference between the phase and density scatterplates is that the SS component of the hotspot term receives a 180° phase shift when a phase scatterplate is used. This is because cosinusoidal phase gratings shift the ±1 diffracted orders by 90° with respect to the undiffracted light and the SS beam (twice scattered) receives a 180° total phase shift. As ϕ varies, the

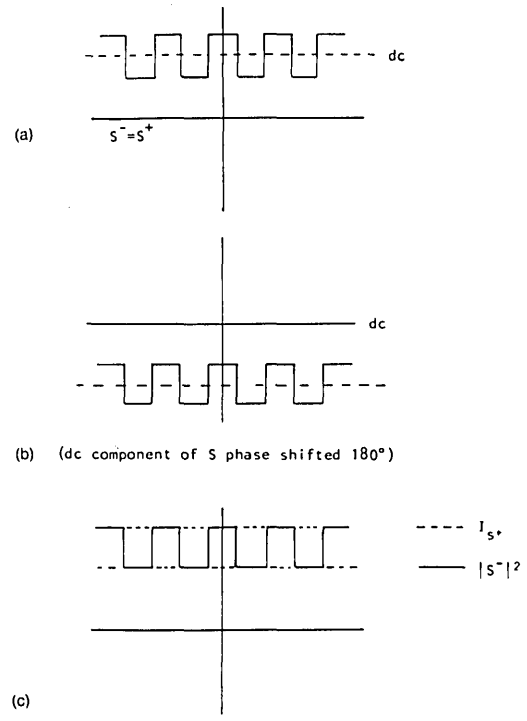

FIG. 5. Simplified view of how the density scatterplate absorbs light.

signal and hotspot intensities will oscillate 180° out of phase. The density scatterplate does not impart these phase shifts to the diffracted light so both the signal and hotspot intensities will be in phase as ϕ is varied. The additional energy must be absorbed by the scatterplate.

Figure 5 shows qualitatively how this occurs. For simplicity the scatterplate amplitude transmission shown in A has a bar target profile so the amplitude and intensity will have the same form. B shows the amplitude just before the second scatterplate passage when $\phi = \pi$. The dc component has been shifted 180° by the PZT mirror and the squared modulus (I_{S^+}) will be contrast reversed as shown in C (the dotted line). When $\phi = \pi$ additional energy is being absorbed in the second passage sine "light" areas of I_{S^+} are falling on "dark" areas of $|S^-|^2$. Mathematically, the analysis goes as the following:

The intensity just before the second plate is

$$I_2^+ = |A(e^{i\phi}t_0 + t_1)|^2 = A^2(t_0^2 + 2t_1t_0\cos\phi + t_1^2). \quad (18)$$

The intensity transmission of the second scatterplate

$$T_2 = A^2(t_0^2 + 2t_1t_0 + t_1^2), \quad (19)$$

so that the energy being absorbed by the scatterplate in both passages is

$$E_S = \int_{AS} (1 - I_2^+T_2)\,dA = A_S - (A_St_0^4 + \langle t_1^4\rangle + 2t_0^2\langle t_1^2\rangle + 4t_0^2\langle t_1^2\rangle\cos\phi) \quad (20)$$

and the sum of E_S and the energy in the image plane

$$E_S + \int_{AS} I_f\,dA = A_S \quad (21)$$

is constant with respect to ϕ.

CONCLUSIONS

In review, the trade off in energy as a null fringe appears across the test lens (signal term equals zero) occurs between the hotspot and the signal in a phase scatterplate. For the density scatterplate, the trade off is between the plate absorption and signal.

The experiment depicted in Fig. 4 was set up and the results stated were found to be correct. One difficulty encountered, however, was intensity modulations caused by light being fed back into the unpolarized laser. False detector signals were recorded at first because this modulation was dependent on piston error. This problem was alleviated by polarizing the laser light from the pinhole and placing a (1/4)λ plate just after the scatterplate to rotate by 90° the plane of polarization of the light being fed back into the laser.

The Fourier optics approach to scatterplate interferometry has enabled us to answer questions concerning energy transfer with piston error. As alluded to earlier however, its use has a wider range of application. Questions on how fringe contrast is affected by pinhole size, reference beam focus, and quality of scatterplate flip symmetry will be discussed in a future paper.

ACKNOWLEDGMENT

The work completed for this paper was funded under Contract No. DAA D07-77-C-0074 for the U.S. Army at White Sands Missile Range, New Mexico.

[1]J. M. Burch, "Scatter Fringe Interferometry," J. Opt. Soc. Am. **52**, 600 (1962).
[2]R. M. Scott, "Scatter Plate Interferometry," Appl. Opt. 8, 531–537 (1969).
[3]J. B. Houston, Jr., "How to Make and Use a Scatterplate In Interferometer," Opt. Spectra 4, 32 (1970).
[4]J. D. Gaskill, *Linear Systems, Fourier Transforms, and Optics* (Wiley-Interscience, New York, 1978) p. 216.